AD-A049 509 MASSACHUSETTS INST OF TECH CAMBRIDGE GAS TURBINE AND--ETC F/G 20/5
FUNDAMENTAL MECHANISMS OF NONEQUILIBRIUM MHD LASING PHENOMENA.(U)
OCT 77 J L KERREBROCK F44620-76-C-0067

UNCLASSIFIED AFOSR-TR-78-0003 NL

| OF |
AD
A049 509

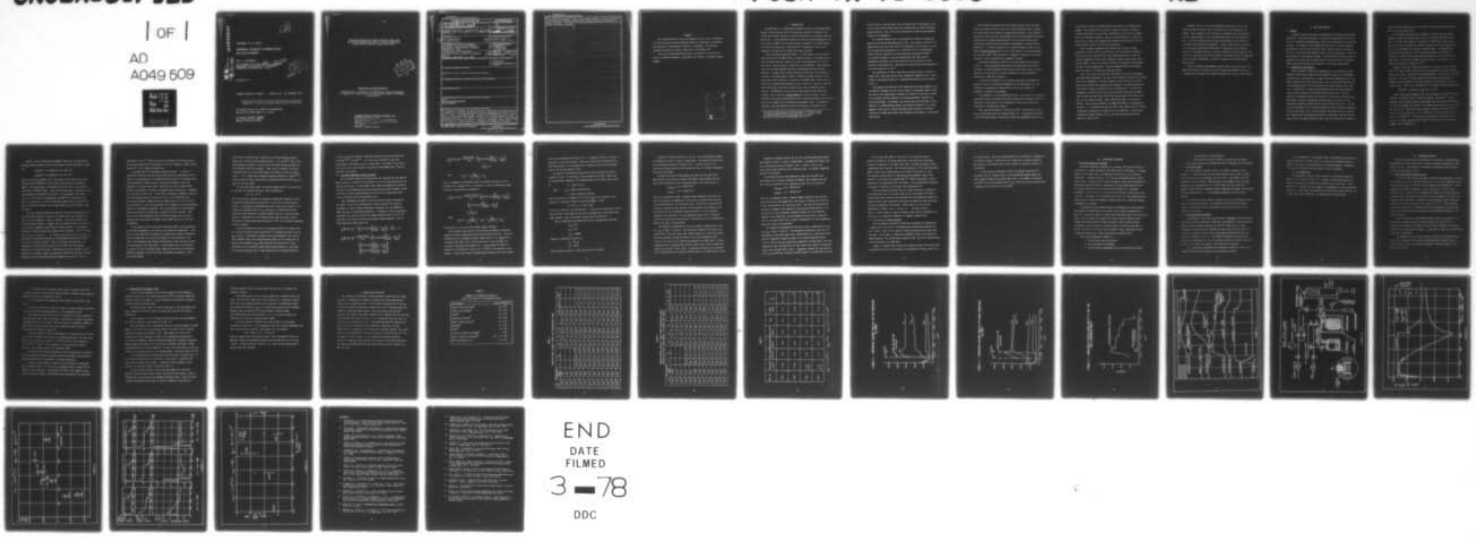

END
DATE
FILMED
3-78
DDC

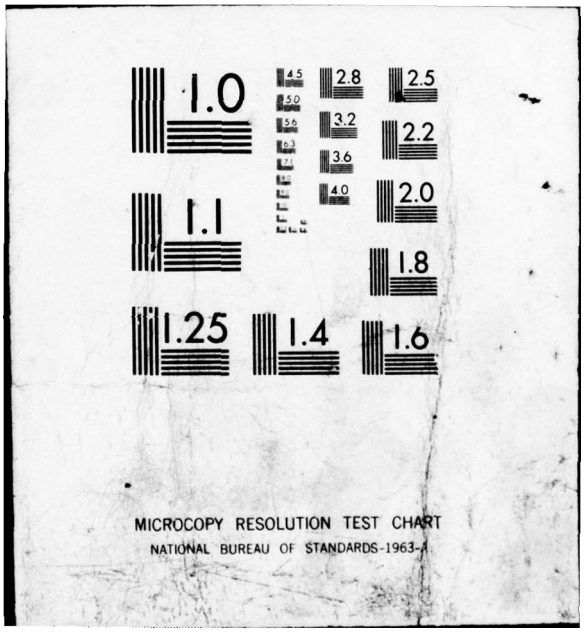
1.0
1.1
1.25
1.4
1.6
1.8
2.0
2.2
2.5
2.8
3.2
3.6
4.0
4.5
5.0
5.6
6.3
MICROCOPY RESOLUTION TEST CHART
NATIONAL BUREAU OF STANDARDS-1963-A

AFOSR-TR- 78-0003

FUNDAMENTAL MECHANISMS OF NONEQUILIBRIUM MHD LASING PHENOMENA

JACK L. KERREBROCK

GAS TURBINE AND PLASMA DYNAMICS LABORATORY
MASSACHUSETTS INSTITUTE OF TECHNOLOGY
CAMBRIDGE, MASSACHUSETTS 02139

OCTOBER 1977

INTERIM SCIENTIFIC REPORT 1 MARCH 1976 - 28 FEBRUARY 1977

AIR FORCE OFFICE OF SCIENTIFIC RESEARCH/NA
BOLLING AIR FORCE BASE, D C 20332

AIR FORCE SYSTEMS COMMAND
UNITED STATES AIR FORCE

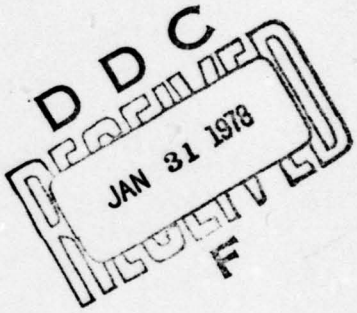

AIR FORCE OFFICE OF SCIENTIFIC RESEARCH (AFSC)
NOTICE OF TRANSMITTAL TO DDC
This technical report has been reviewed and is approved for public release IAW AFR 190-12 (7b).
Distribution is unlimited.
A. D. BLOSE
Technical Information Officer

UNCLASSIFIED

SECURITY CLASSIFICATION OF THIS PAGE (When Data Entered)

REPORT DOCUMENTATION PAGE	READ INSTRUCTIONS BEFORE COMPLETING FORM
1. REPORT NUMBER (19) AFOSR-TR-78-0003	2. GOVT ACCESSION NO. / 3. RECIPIENT'S CATALOG NUMBER (9)
4. TITLE (and Subtitle) (6) FUNDAMENTAL MECHANISMS OF NONEQUILIBRIUM MHD LASING PHENOMENA.	5. TYPE OF REPORT & PERIOD COVERED INTERIM rept. 1 Mar 76 - 28 Feb 77
	6. PERFORMING ORG. REPORT NUMBER
7. AUTHOR(s) (10) JACK L. KERREBROCK	8. CONTRACT OR GRANT NUMBER(s) (15) F44620-76-C-0067 new
9. PERFORMING ORGANIZATION NAME AND ADDRESS MASSACHUSETTS INSTITUTE OF TECHNOLOGY ✓ GAS TURBINE & PLASMA DYNAMICS LABORATORY CAMBRIDGE, MA 02139	10. PROGRAM ELEMENT, PROJECT, TASK AREA & WORK UNIT NUMBERS (16) 2308 C1 (17) 61102F
11. CONTROLLING OFFICE NAME AND ADDRESS AIR FORCE OFFICE OF SCIENTIFIC RESEARCH/NA (11) BLDG 410 BOLLING AIR FORCE BASE, D C 20332	12. REPORT DATE Oct 77 (12) 45 p. 13. NUMBER OF PAGES
14. MONITORING AGENCY NAME & ADDRESS (if different from Controlling Office)	15. SECURITY CLASS. (of this report) UNCLASSIFIED
	15a. DECLASSIFICATION/DOWNGRADING SCHEDULE

16. DISTRIBUTION STATEMENT (of this Report)

Approved for public release; distribution unlimited.

17. DISTRIBUTION STATEMENT (of the abstract entered in Block 20, if different from Report)

18. SUPPLEMENTARY NOTES

19. KEY WORDS (Continue on reverse side if necessary and identify by block number)

LASER
MHD (MAGNETOHYDRODYNAMICS)
PLASMA DYNAMICS

20. ABSTRACT (Continue on reverse side if necessary and identify by block number)

The fundamental mechanisms of lasing phenomena in MHD lasers are being studied by a combination of numerical modeling and a pulsed experimental simulation of the MHD flow laser. The numerical model includes all phenomena known to be of importance in nonequilibrium MHD plasmas, as well as the molecular kinetics of CO_2 excitation and lasing. The kinetics of growth of ionization and of electrothermal instabilities are treated in detail. Except for the magnetic field, which is low by a factor of 4, these conditions are appropriate for MHD laser operation. The high magnetic field required for UxB induced lasing should not reduce the gain.

DD FORM 1 JAN 73 1473 EDITION OF 1 NOV 65 IS OBSOLETE

UNCLASSIFIED

SECURITY CLASSIFICATION OF THIS PAGE (When Data Entered)

410 554

and probably will increase it for a given current density. It is concluded that plasma conditions suitable for MHD laser operation have been achieved in the pulsed simulation. The numerical modeling indicates that these conditions can be reached in an MHD flow laser.

FOREWORD

This interim scientific report was prepared by Prof. Jack L. Kerrebrock of the Gas Turbine and Plasma Dynamics Laboratory, Department of Aeronautics and Astronautics, Massachusetts Institute of Technology. The work was accomplished during the period 1 March 1976 to 28 February 1977.

This work is being administered under the direction of the Air Force Office of Scientific Research, supervised by Dr. Bernard T. Wolfson, Program Manager.

I. INTRODUCTION*

The MHD laser is a nonequilibrium generator in which the disequilibrium between the electron gas and the translational degrees of freedom of the carrier gas is used to produce a population inversion in a molecular additive, such as CO_2. As the difference between the electron and gas temperatures can be as large as 3000°K, and the power density, measured by the Joule heating rate, also very large (up to 500 watts/cm^3 in generators), there is the possibility of gain and very high lasing power densities.

There are several appealing features of this concept. As the electric power generated by the MHD process is delivered locally to the molecular gas, entirely within the flow, there is no need to take high powers out of the power source, and in turn put it back into a gas discharge. This eliminates many uncertainties stemming from power conditioning and from electrode phenomena. Further, while a high speed gas flow may have to be provided in an electric discharge laser in order to remove the energy rejected to the lower laser level, this flow is intrinsic to the MHD laser. The process for inversion production being essentially local, there is a chance of achieving more uniform gain, hence better beam quality than in externally excited devices. Consideration of the potential efficiencies of MHD lasers must recognize that it converts thermal energy into optical energy. Various estimates have placed the efficiency of such conversion between 3 and 5 percent. This is much higher than is achieved by gas dynamic lasers. Although gas discharge lasers may approach 20 percent efficiency of conversion from

---

* The serious reader will note that the initial paragraphs of this introduction are identical to those of Ref. 1. It is felt they are needed because of the arcane nature of the subject. New aspects of the work are discussed on pp. 3-5.

electric power to optical power, this efficiency must be multiplied by that of the electric power system (and power conditioning) for which 25 percent seems optimistic. Thus, the overall efficiencies of MHD and gas discharge lasers may be comparable.

The research reported here is an outgrowth of research on high power density nonequilibrium MHD generators at MIT. This research has led to the demonstration that very high levels of dissipation can be achieved in supersonic nonequilibrium generators, up to 500 watts cm^{-3}, with differences between electron temperature and gas temperature approaching 3000°K.[2] In a parallel program, it was also demonstrated that high levels of vibrational excitation, near equilibrium with the electron gas, can be achieved in such generators. Excitation of carbon monoxide was demonstrated in the MIT generator in 1969.[3]

The possibility of direct excitation of molecular gases to produce a single-cavity high power density laser immediately suggested itself. Such a concept, using carbon dioxide in a cesium-helium plasma has been analyzed in Ref. 4.

The analysis and experience with nonequilibrium plasmas suggested that the physical phenomena of such a device might be exceedingly complex, since the kinetic and thermochemical complexity of molecular excitation is added to the already intricate behavior of the electrothermally unstable nonequilibrium plasma. Accordingly, the present study was undertaken, of the behavior of a nonequilibrium plasma, with molecular addition, in a strong magnetic field, but in a pulsed experiment which stimulates the kinetic situation of an MHD laser without the complexity and expense of a high speed flow system.

The technique of modeling the flow-induced electric field of an MHD laser by an applied electric field has the great advantage that it enables the uncoupling of fluid dynamic and bulk plasma phenomena. This technique was used to obtain the first experimental data on electrothermal (ionization) instabilities in nonequilibrium plasmas,[5] and this data has since been correlated by theory[6] and corroborated by measurements in nonequilibrium generators.[7] A further advantage of the pulsed technique is that the very complex kinetic processes which occur in the plasma as it flows downstream in the actual laser, are displayed as a (temporal) transient in the pulsed experiment, vastly simplifying the diagnostic problem.

Preliminary experiments carried out by this technique were reported in Ref. 8. These experiments demonstrated the usefulness of the pulsed technique, and also demonstrated gain and net power output from a Cs seeded mixture of He, CO_2 and N_2 at electron densities and current densities appropriate to MHD laser operation.

A theoretical treatment[9] of the physical processes in the MHD laser produced results in qualitative agreement with the experiments, but overestimated the importance of deexcitation of Cs by CO_2, leading to a pessimistic estimate of performance.

The purposes of the work described here are: 1) to carry out a systematic experimental study of the gain and optical properties of plasmas suitable for MHD lasers, and 2) based on this information to carry out a feasibility assessment of the MHD laser concept.

Since the last reporting of this work in Ref. 1, the results of a major study of MHD lasers have been reported in Ref. 10. A theoretical evaluation of the MHD laser concept is presented, along with experimental results from

flow systems in which $\underline{U} \times \underline{B}$ induced gain was observed in Cs seeded He-CO_2 plasmas. The results were very erratic, evidently because of chemical reaction between the Cs and the CO_2, and difficulty with the salt windows, which were chemically attacked. This led the investigators to substitute Xe for Cs as a seed; they acquired more consistent data but gain only with applied electric fields, not with $\underline{U} \times \underline{B}$ excitation.

There is general agreement that the MHD laser requires a plasma composition of about 10^{-2} CO_2 and 10^{-5} Cs in He for successful operation. The CO_2 fraction is limited by the Joule heating available to raise the electron temperature to the levels required to pump the upper laser level (around 2500°K). The Cs is needed to provide the required electron density at these electron temperatures. This gas composition poses two problems which are unique to the MHD laser among CO_2 lasers.

First, the low CO_2 concentration and absence of N_2 alter the pumping and deactivation mechanisms. The upper level pumping is directly by electrons and is well understood.[4] In most treatments of CO_2 lasers the two lower levels (100 and 010) have generally been assumed to be tightly coupled and deactivated by atomic collisions (by He in the MHD laser). We find this assumption is invalid at the low CO_2 concentrations required by the MHD laser because the lower laser level (100) is deactivated by collision with CO_2, the rate being limiting. Thus a three-level model is required for the CO_2. Such has been included in the MHD laser model to be discussed in Section II. It is shown there that the (100 → 010) transfer rate is critical to MHD laser performance, if lasing at 10.6 μ is required. It may be that the MHD laser should operate at 9.6 μ, but this question has not been explored in depth as yet.

Secondly, the low Cs fraction and chemical reactivity of Cs and CO_2 raise the question whether these two species can in fact coexist in the plasma. Early estimates of the reaction rate suggested that they could for the flow times required in full scale MHD lasers such as were projected in Ref. 4, but the reaction has led to great uncertainties in the results of all small scale feasibility experiments. Indeed a great deal of the effort of the research described here has gone to developing the gas handling system for the pulsed apparatus so that the chemical reaction between Cs and CO_2 can be controlled, and that the amount of Cs present during the experiment can be accurately determined. Section III presents the methods evolved, which do work.

Section IV presents experimental results, which include the gain of the MHD laser plasma as a function of current density and magnetic field, and transient data from which the (100-010) transfer rate in CO_2 can be inferred.

II. MHD LASER MODELING

2.1 Summary

A computer program describing the performance of an MHD laser has become operational. The program combines a previously developed model of the fluid flow in a nonequilibrium MHD generator with a new description of CO_2 molecular kinetics. The results of this program indicate that in a laser containing one percent or less of CO_2 the optical power extraction rate is limited by the rate at which the 10°0 symmetric stretch level is deactivated to the 01'0 bending level by collisional processes. This relaxation proceeds an order of magnitude more slowly than the deactivation of the 01'0 level to the ground state, which had previously been assumed to be the rate-limiting step.

2.2 Discussion of CO_2 Kinetics

Previous analyses of MHD lasers employing CO_2 as the optically active molecular species have assumed that the symmetric stretch (ν_1) and bending (ν_2) modes are in equilibrium at a single vibrational temperature due to the Fermi resonance that exists between them. As it is well known that the rate of deactivation of the 01'0 via collisions with helium atoms is very rapid ($\simeq 5.0 \times 10^6 \text{atm}^{-1}\text{sec}^{-1}$), such a strong coupling between the modes implies a rapid removal of molecules from the 10°0 lower laser level. This has important consequences during the extraction of optical power from the laser gain medium, because it establishes an upper limit on the rate at which stimulated transitions between the 00°1 and 10°0 levels can occur. If this rate of production of 10.6 μ photons exceeds the rate of removal of molecules from the lower laser level, the population of the lower level will build up very rapidly until the population inversion is destroyed. Then the optical power that can be removed from the laser, given by the energy per transition

times the photon production rate, is limited by the collisional deactivation rate of the lower laser level.

For conditions under which the assumption of strong coupling between symmetric stretch and bending modes is valid, the known rapid deactivation rate of the 01'0 level leads to a prediction of high optical power output. This prediction is confirmed by the high continuous wave power obtained from $CO_2 - N_2 - He$ gas dynamic and electric discharge lasers. The assumption of equilibrium between modes ν_1 and ν_2 has always seemed valid because the performance of these lasers closely matched prediction,[13] and because of the measurement of this rate by Rhodes, Kelly and Javan, which implied a very strong coupling ($\cong 3.0 \times 10^8 atm^{-1} sec^{-1}$).[14]

However, more recent studies have reported a variety of slower coupling rates,[15-22] most of them slower by an order of magnitude than the RKJ (Rhodes, Kelly, Javan) rate. Bulthuis[19] performed experimental studies of the coupling process in a $CO_2 - N_2 - H_2O$ laser plasma which indicated that equilibrium between ν_1 and ν_2 existed if the CO_2 concentration exceeded 12% of the H_2O concentration. From this he concluded that the primary coupling mechanism was

$$CO_2(10°0) + CO_2(00°0) \rightleftarrows 2CO_2(01'0) + 54\ cm^{-1}$$

These studies were extended to $CO_2 - N_2 - He$ plasmas by Stark,[20] by Murray, Mitchner, and Kruger,[22] and by Jacobs, Pettipiece, and Thomas.[21] Based on momentum transfer considerations, Stark argues that the relative effectiveness of collision partners for the 10°0 ~ 01'0 deactivation process is 1:0.46:0.054 for $CO_2 : N_2 : He$. Using this estimate, Murray, Mitchner and Kruger report a value for the $CO_2 - CO_2$ rate of $9.1 \times 10^5 atm^{-1} sec^{-1}$, while the $CO_2 - He$ rate is $4.9 \times 10^4 atm^{-1} sec^{-1}$. If only $CO_2 - CO_2$ collisions are effective in this process, as Rosser, Hoag and Gerry report,[18] the $CO_2 - CO_2$ rate is slightly higher, $1.52 \times 10^6 atm^{-1} sec^{-1}$.

Finally, Jacobs, Pettipiece and Thomas[21] report that the deactivation process actually proceeds via two or more steps, the most important of which are:

$$CO_2(10°0) + M \rightleftarrows CO_2(02°0) + M + 102.8\ cm^{-1}$$

$$CO_2(02°0) + M \rightleftarrows CO_2(01'0) + M + 50.1\ cm^{-1}$$

where M is either $CO_2(00°0)$ or He. They report a very rapid rate for the first process ($\simeq 10^8 atm^{-1} sec^{-1}$ for both $CO_2 - CO_2$ and CO_2 - He collisions). However, the second step of the process was found to have a rate about ten times slower ($\simeq 10^7 atm^{-1} sec^{-1}$). This is of the same order of magnitude as the rate determined by Seeber[16] for the 10°0 - 01'0 relaxation, and within a factor of ten of the rate determined by Bulthuis[19] for this process in a $CO_2 - N_2 - H_2O$ mixture. It is 60 to 100 times larger than the rate given by Murray, Mitchner and Kruger, but 10 times slower than that of Rhodes, Kelly and Javan.

The first conclusion that may be drawn is that the detailed kinetics of the collisional relaxation process of the lower laser level $CO_2(10°0)$ are still not well understood. There is, however, a wide body of theoretical and experimental evidence to suggest that the relaxation rate is from one to three orders of magnitude slower than previously believed. A preliminary measurement from the present work supports this conclusion. It and the other data are listed in Table 1. The evidence also indicates that the CO_2- CO_2 collisions are much more effective in this relaxation process than either CO_2 - He or $CO_2 - H_2O$ collisions. Then, for low CO_2 concentrations, the relaxation of the 01'0 level by H_2O or He is faster than the coupling between the 10°0 and 01'0 levels. This does not pose any problems for most high power CO_2 lasers, because they generally operate with CO_2 mole fractions between 5 and 15%, and H_2O/He fractions between 10 and 15%, the balance

being made up of N_2.[13] Thus the criterion of Bulthuis that the CO_2 concentration must exceed 12% of the fraction of the 01'0 relaxant in order to have strong 10°0 - 01'0 coupling is easily met.

In the MHD laser a far different situation prevails. A study by Lowenstein[9] indicates that the CO_2 concentration must be kept below 0.1% in order to avoid quenching of the excited electronic states of the alkali seed, thus depressing the number density of electrons required to excite CO_2 molecules to the upper laser level. While this low limit resulted from a probable overestimate of the CO_2 - Cs quenching cross section, Ref. 4 indicates a CO_2 fraction of about 0.01. In this case, according to Bulthuis' criterion, the rate-limiting process is actually the 10°0 - 01'0 relaxation rate. All previous analyses of MHD lasers have assumed this rate to be very fast, as noted earlier, so that the populations of the symmetric stretch and bending modes are in Boltzmann equilibrium. With this assumption the rate-limiting process is naturally the relaxation of CO_2(01'0) by He collisions. Thus, there is the clear possibility that the previous analyses may have overestimated the optical power obtainable from an MHD laser by up to an order of magnitude.

In the present analysis the three vibrational modes of the CO_2 molecule are treated independently, each with its own vibrational temperature. Since all the other collisional and radiative transfer rates between the modes are known to within 20%, we can study the effects of the uncertainty in the 10°0 - 01'0 relaxation rate without accumulating too much inaccuracy because of uncertainties in the other rates. In the present report we illustrate the results for the two extreme cases, namely the very slow rate of Murray, Mitchner and Kruger, and the very fast rate implied by assuming ν_1 and ν_2 are in equilibrium.

the electron continuity (rate) equation, the electron momentum equation (Ohm's Law), and the electron energy equation. It is known[25,6] that if the Hall parameter β exceeds a critical value, the plasma becomes unstable and electrothermal waves may propagate. These result in temporal and spatial nonuniformities in n_e and T_e which reduce the values of β and the conductivity σ. By a quasi-linear averaging technique developed by Solbes[6,26,27] we may account for these reductions by calculating effective values β_{eff} and σ_{eff} for the bulk plasma.

In this quasi-linear model the electron number density is first written as the sum of an average term plus a small perturbation:

$$n_e = \langle n_e \rangle (1 + \eta)$$

The three electron equations are themselves averaged and combined to yield an expression describing the evolution of $\langle n_e \rangle$ as the flow moves down the channel. By assuming the nonuniformities have a plane wave structure it is possible to determine values of σ_{eff} and β_{eff} for calculating the joule dissipation which appears in the heat transfer term of the electron energy equation. Manipulation of the averaged plasma equation yields a second differential equation describing the growth of $\langle \eta^2 \rangle$, the fluctuation parameter, with flow distance.

A previous numerical solution of the fluid equations for the MHD laser by the United Aircraft Research Laboratory[11,12] assumed functional forms for σ_{eff} and β_{eff}. Furthermore, constant values were assumed for the critical Hall parameter (above which nonuniformities develop in the plasma) and the apparent Hall parameter β_{app} (which describes the reduction from ideal performance due to generator loading effects and interelectrode shorting). In the present analysis each of these quantities is calculated explicitly

at every step in the numerical integration using the reduction formulas due to Solbes[6,26,27] and Cole.[24] It is felt that this gives a more exact description of the plasma state on a local level. The values of $\langle n_e \rangle$ and T_e that result give a more accurate calculation of the pumping rate of the CO_2 molecules by electrons.

2.3 Coupling of MHD Model with CO_2 Kinetics

The new kinetic model of the CO_2 molecule was combined with the improved MHD flow model to calculate the excitation rate of the lasing species and the optical power output. In the present study computer programs were developed for both the two-temperature and three-temperature CO_2 kinetic models, so that the effects of weak coupling between the 10°0 and 01'0 vibrational levels could be compared with the equilibrium result.

From a mathematical viewpoint the most obvious difference between the two models is that the three-temperature version requires the numerical integration of seven ordinary differential equations; the two-temperature model has only six differential equations. In addition to the two gasdynamic equations (for p_0 and T_0) and the two plasma equations (for $\langle n_e \rangle$ and $\langle \eta^2 \rangle$), each model must solve a set of CO_2 vibrational energy equations. For the three-temperature model these are:

$$\frac{1}{A_D}\frac{d}{dx}\left(E_1 U A_D\right) = -\left[E_1(T_1)-E_1(T_2)\right]\left(\frac{1}{\tau_{1He}}+\frac{1}{\tau_{1CO_2}}\right)+\frac{\nu_3}{\nu_3-\nu_1}\,g\,I$$

$$\frac{1}{A_D}\frac{d}{dx}\left(E_2 U A_D\right) = \frac{E_2(T_e)-E_2(T_2)}{\tau_{2e}}+\left[E_3(T_3)-E_3(T_2)\right]\left(\frac{1}{\tau_{3He}}+\frac{1}{\tau_{3CO_2}}\right)$$
$$+\left[E_1(T_1)-E_1(T_2)\right]\left(\frac{1}{\tau_{1He}}+\frac{1}{\tau_{1CO_2}}\right)$$
$$-\left[E_2(T_2)-E_2(T)\right]\left(\frac{1}{\tau_{2He}}+\frac{1}{\tau_{2CO_2}}\right)$$

$$\frac{1}{A_D}\frac{d}{dx}\left(E_3 U A_D\right) = \frac{E_3(T_e)-E_3(T_3)}{\tau_{3e}} - \left[E_3(T_3)-E_3(T_2)\right]\left(\frac{1}{\tau_{3He}} + \frac{1}{\tau_{3CO2}}\right) - \frac{\nu_1}{\nu_3 - \nu_1} g I$$

where $$E_i(T_j) = \frac{n\nu_i}{e^{n\nu_i/k T_j} - 1} n_{CO_2}$$

and T_{ij} represents the relaxation time of a molecule in mode i due to a collision with a member of the j th species. In the two-temperature model the first two equations are combined as

$$\frac{1}{A_D}\frac{d}{dx}\left(E_{12} U A_D\right) = \frac{E_{12}(T_e)-E_{12}(T_2)}{\tau_{2e}} + \left[E_3(T_3)-E_3(T_2)\right]\left(\frac{1}{\tau_{3He}} + \frac{1}{\tau_{3CO_2}}\right) - \left[E_{12}(T_2)-E_{12}(T)\right]\left(\frac{1}{\tau_{2He}} + \frac{1}{\tau_{2CO_2}}\right) + \frac{\nu_3}{\nu_3 - \nu_1} g I$$

where $$E_{12}(T_i) = \frac{n\nu_1}{e^{n\nu_1/k T_i} - 1} n_{CO_2} + \frac{2n\nu_2}{e^{n\nu_2/k T_i} - 1} n_{CO_2}$$

The equation for the upper level energy remains unchanged.

We now present some results of calculations performed for identical geometries and gas compositions using the two different models. The flow is assumed first to be expanded through a wedge nozzle 5 cm in length with a divergence half angle of 10.7° and an area ratio at the exit $\frac{A_e}{A^*} = 5.6$, yielding an isentropic Mach number of 4. In this region the fluid is assumed to be preionized so that $n_e = 8.5 \times 10^{18} m^{-3}$ at the entrance to the channel. The gas next enters the wedge-shaped channel section with a width

of 54 cm and divergence half angle of 0.3°. A magnetic field of 4.0 tesla is initiated 1 cm into the channel. Mirrors of reflectivity 0.98 and 0.95 are positioned parallel to the channel axis, creating an optical axis perpendicular to the flow and magnetic field.

The logic of the program is structured so that initially the optical intensity is zero. At each point in the integration the small signal gain is calculated and compared to the threshold gain for the laser cavity, given by

$$g = -\frac{1}{2L} \ln (r_1, r_2)$$

where r_1, r_2 = Mirror Reflectivities

L = Mirror Separation Distance

When this quantity is exceeded for the first time, the calculation of the intensity is initiated, based on the condition $\frac{dg}{dx} = 0$, where

$$g = g\ (I,\ T_e,\ T,\ T_{100},\ T_{001})$$

is the local value of the saturated gain. In this way the extraction of power from the laser cavity begins as soon as the pumping rate of the upper laser level reaches a value that pushes the gain above the threshold.

The gas composition considered here has the following mole fractions:

$$x_{CO_2} = 0.01$$

$$x_{Cs} = 10^{-5}$$

$$x_{He} = 0.98999$$

Stagnation conditions are given by:

$$P_0 = 20 \text{ atm}$$

$$T_0 = 2090°K$$

These conditions result in a mass flow rate of 1.56 kg/sec.

Temperature response profiles for the two- and three-temperature models are presented in Figs. 2.1 and 2.2 respectively. The numerical results from the calculations are given in Tables 2 and 3. Finally, plots of the local optical power density gI are included as Fig. 2.3, giving a comparison between the two models.

Calculations with the three-temperature model use the lower level deactivation rate of Murray, Mitchner and Kruger, which assumes that both CO_2 and He are involved in the relaxation process, with rates given by:

$$k_{100\text{-}CO_2} = 8.8 \times 10^5 \text{atm}^{-1}\text{sec}^{-1}$$

$$k_{100\text{-He}} = 4.8 \times 10^4 \text{atm}^{-1}\text{sec}^{-1}$$

This set of parameters yields a somewhat higher relaxation rate than that given by Bulthuis, who assumed that only CO_2-CO_2 collisions were effective in the deactivation of the lower laser level. This does not seem entirely realistic, although it does indicate the much greater effectiveness of the CO_2 molecule in the collisional relaxation process. For the conditions assumed in this simulation, the two-temperature model gives a relaxation time for the lower laser level of about 1 microsecond; the three-temperature model gives about 10 microseconds.

The immediate consequences of this can be seen by examining the curves for T_{100} in Figs. 2.1 and 2.2. The vibrational temperature (and hence the population) of the lower laser level remains hung up at a high value during and after expansion through the nozzle in the three-temperature model. In fact, with the low CO_2 concentration employed in the MHD laser, the three-temperature model indicates that the lower laser level actually relaxes more slowly than the upper (00°1) level. A population inversion is not possible until CO_2 molecules get excited by electron impact in the MHD channel section.

Temperature response profiles for the two- and three-temperature models are presented in Figs. 2.1 and 2.2 respectively. The numerical results from the calculations are given in Tables 2 and 3. Finally, plots of the local optical power density gI are included as Fig. 2.3, giving a comparison between the two models.

Calculations with the three-temperature model use the lower level deactivation rate of Murray, Mitchner and Kruger, which assumes that both CO_2 and He are involved in the relaxation process, with rates given by:

$$k_{100\text{-}CO_2} = 8.8 \times 10^5 \text{atm}^{-1}\text{sec}^{-1}$$

$$k_{100\text{-He}} = 4.8 \times 10^4 \text{atm}^{-1}\text{sec}^{-1}$$

This set of parameters yields a somewhat higher relaxation rate than that given by Bulthuis, who assumed that only CO_2-CO_2 collisions were effective in the deactivation of the lower laser level. This does not seem entirely realistic, although it does indicate the much greater effectiveness of the CO_2 molecule in the collisional relaxation process. For the conditions assumed in this simulation, the two-temperature model gives a relaxation time for the lower laser level of about 1 microsecond; the three-temperature model gives about 10 microseconds.

The immediate consequences of this can be seen by examining the curves for T_{100} in Figs. 2.1 and 2.2. The vibrational temperature (and hence the population) of the lower laser level remains hung up at a high value during and after expansion through the nozzle in the three-temperature model. In fact, with the low CO_2 concentration employed in the MHD laser, the three-temperature model indicates that the lower laser level actually relaxes more slowly than the upper (00°1) level. A population inversion is not possible until CO_2 molecules get excited by electron impact in the MHD channel section.

On the other hand, Table 2 shows that the two-temperature model predicts some gain in the nozzle region due to the selective vibrational freezing of molecules in the upper laser level, the same principle by which a gasdynamic laser operates. The low gain prediction of the three-temperature model, valid at CO_2 concentrations on the order of one percent or less, has important implications for high-pressure CO_2 gasdynamic lasers which operate in a so-called "CO_2-starved" mode.[28] Indeed, measurement of small-signal gain in a gasdynamic laser with 99% He - 1% CO_2 composition represents one method of checking the slow lower level relaxation rate.

Since the induced transition rate in a laser oscillator is limited by the deactivation rate of the lower laser level, we can expect that with a deactivation time of almost 10 microseconds the three-temperature model will predict optical power production rates about ten times less than those given by the two-temperature calculations. This is seen to be the case by examination of Tables 2 and 3, and Fig. 2.3. The abrupt bumps in Figs. 2.1 and 2.3 appear to have no physical cause; they are believed to be the result of a numerical instability or computer roundoff error.

2.4 Directions for Further Research

With the computer simulation of MHD laser performance now operational, a program can be carried out to determine more optimal design features for such a device. Thus far our choice of operating conditions has been rather arbitrary. We are about to undertake a parametric study of the effects of channel geometry, CO_2 concentration, magnetic field, and mirror reflectivities on the performance of an MHD laser.

However, it appears that the two most critical factors are the CO_2 (10°0) relaxation rate and the cross section for quenching of the $6P_{1/2}$ state of Cs

by CO_2 encounters. Each of these quantities will be treated as a parameter in the computer program. Several runs will be made over a range of values of each quantity to determine which, if any, permit the practical operation of an MHD laser.

It would clearly be desirable to find a gas additive that does not seriously upset the energy balance in the non-equilibrium MHD plasma, and which rapidly relaxes the CO_2 lower laser level. For example, it has been reported[18] that the deactivation rate of CO_2 (10°0) by Xe is of the same order of magnitude as the rate due to CO_2 itself.

III. EXPERIMENTAL PROCEDURE

3.1 The Pulsed Simulation Technique

The pulsed experiment simulates by a transient the convected history of the fluid as it passes through the high speed flow of an MHD laser. In earlier phases of the present work, the transient was used only in the electrical conditions. A steady flow of He + Cs + CO_2 was established through a quartz test section. A pulsed electric field and magnetic field then established the MHD plasma conditions desired. Experience with this system showed that the Cs concentration could not be controlled well enough to do a systematic experiment. The reaction of Cs and CO_2 made the actual Cs concentration very uncertain. Furthermore, the continuous flow of He + Cs + CO_2 through the test section quickly coated the diagnostic windows and mirrors, requiring frequent disassembly for cleaning.

Accordingly the gas handling system was redesigned for pulsed operation. The sequence of events which occur during a test is shown schematically in Fig. 3.1. Helium is stored in a heated flask containing copper wool wet with Cs. When a valve is opened this mixture blows down to vacuum through the test chamber giving the pressure transient sketched. Near the peak pressure, the magnetic field is pulsed on, and the shutter on the CO_2 probe laser is opened. Finally, the electric field is pulsed to pass a prescribed current through the plasma after a short electrostatic preionizer pulse.

The critical diagnostics consist of:

1. The CO_2 probe laser and detector.
2. The Cs absorption measurement.
3. Electron density measurement by the Cs bound-free continuum.

4. CO measurement by line absorption.

5. Hall and axial fields by probes in contact with the plasma.

Some unusual features of the apparatus will be discussed in the following.

3.2 Pulsed Flow System

The flow system is sketched in Fig. 3.2. Before a series of tests, liquid Cs is flushed through the right hand stainless steel vessel (of about 0.3 ℓ capacity) so as to thoroughly wet the Cu wool. The liquid Cs is then returned to the left vessel. During operation the pneumatic valve is opened allowing the He saturated with Cs to flow through the test section for a period of about 700 ms, the maximum pressure being about 63 mm Hg. This provides reliable seeding with Cs. It also minimizes fogging of the test section windows.

To minimize the Cs-CO_2 chemical reaction, the CO_2 is introduced as shown, into the flowing He-Cs mixture, the operation of the solenoid valve being timed to coincide with that of the pneumatic valve so as to give a nearly constant CO_2 fraction.

3.3 Cs Concentration Measurement

Determination of the actual concentration of metallic Cs in the discharge has been especially troublesome in MHD laser investigations. Here the measurement is done by resonance absorption at 4550 Å of light from a Cs lamp. To minimize noise and record a reference on each scope trace the light from the lamp is chopped at about 15 kHz, giving many periods during a gas flow pulse, as indicated in Fig. 3.1. The change in height of the pulses gives directly the absorption by the Cs in the tube, and since the record spans the whole gas flow time, any fogging of the windows can be detected.

The Cs absorption measurement was calibrated by means of a quartz test chanber sealed off with 60 mm Hg of He and heated in an oven.

In the experiments to be described below, the discharge occurred late in the gas flow pulse, as shown in Fig. 3.1, where the Cs absorption was very small, so that the Cs concentration was not directly measured. Estimates of its value were inferred from other data, as will be explained.

3.4 CO_2 Probe Laser

The measurement of gain is done by means of a three-pass probe laser beam at 10.6 μ as shown in Fig. 3.3. A shutter is opened just before the electric field pulse to establish the detector zero for each test. As the detector is AC coupled, the gain signal is superimposed on a decay as sketched in Fig. 3.1. The overall time resolution of the system is better than 0.1 μs, a point which will be important in interpretation of the gain data.

IV. EXPERIMENTAL RESULTS

With the above described modifications to the appratus, consistent gain measurements have been achieved over a range of conditions appropriate to MHD lasing operation. The results are conveniently divided into those obtained without, and with magnetic field.

4.1 Measurements Without Magnetic Field

To check the flow system, discharge circuits and instrumentation, a series of experiments was first conducted without CO_2, i.e. with a Cs seeded He plasma. The current was about 0.5 amp cm^{-2} and the conductivity 0.093 mho cm^{-1}. The Cs absorption measurement indicated a Cs mole fraction of 1.0×10^{-4} at the pressure peak. If there were no mechanisms for removal of Cs from the mixture, we would expect this same mole fraction of Cs in the plasma at the time of the discharge some 100 ms later. Analysis of the conductivity results indicated that the Cs mole fraction was in fact closer to 2×10^{-5}. This calculation consisted essentially in estimating the electron temperature, then inferring the Cs concentration from the conductivity, which depends principally on the electron density.

There is therefore some mechanism acting to remove the metallic Cs from the plasma, the time constant for removal being of the order of 35 ms. Whether this mechanism is oxidation by traces of air, diffusion to the walls, or some other is not known at present. In any case, it seems to be reproducible, hence can be dealt with.

Upon addition of CO_2 to a mole fraction of 0.0074 in the He-Cs mixture with a total pressure of 53.8 mm Hg, gain was measured as shown in Fig. 3.3 as a function of time. The principal features of this time history of the gain are as follow:

a. The gain rises in a time of about 10 μs to a value of 0.08 cm^{-1}, is nearly constant for some 100 μs, then decreases, becoming strongly negative before the current is terminated at 330 μs.

b. The negative gain (absorption) then relaxes on about 500 μs time scale.

It should be noted first that the current is actually constant from about 1 μs on, the initial rounding being due to the measurement system.

The decrease of gain from 100 μs on is believed to be due to pumping of the lower laser level (100) by electrons. As this level is heavily populated, it absorbs the 10.6 μ probe beam. When the current is terminated, pumping of this level by electrons stops also and its population decays, giving a corresponding reduction in absorption.

This decay therefore yields a measurement of the deactivation of the 100 level by both 100-020 collisions and by the 100-He mechanism. The decay time being ≈50 μs and the CO_2 pressure ≈5 x 10^{-4} atm we find a rate constant of 4 x 10^{7} $atm^{-1}s^{-1}$, which is to be compared to the values given in Table 1. It falls in the general range of the published values.

It should be noted that measurement of the CO concentration by emission at a line showed no significant amount during the discharge, indicating that CO_2 dissociation did not contribute to the gain termination.

A series of measurements at different current densities yielded peak gains as shown in Fig. 3.4, there being a maximum at about 0.4 amp cm^{-2} for this set of gas conditions. The peak gain is close to the computed values cited in Section II, however larger values have been measured, as noted below.

4.2 Measurements with Magnetic Field

A set of three experiments with different magnetic field strengths is presented in Fig. 3.5, the current and electric field in the upper frames and the 10.6 μ gain at the bottom. As noted previously, the current is actually a square pulse on this time scale.

The axial electric field (in current direction) is initially high as the CO_2 is pumped, and the gain rises on the same time scale that the electric field falls.

For zero magnetic field for these conditions the gain then goes negative on a 100 μs time scale, then relaxes as in Fig. 3.3.

When the magnetic field is increased from zero, the gain displays a pulsed behavior, the time scale for the pulses being of the order of 10 μs, and the amplitude increasing with magnetic field. This appears to be due to the Lorentz force, which generates a pressure wave propagating perpendicular to the current and magnetic field and (probably) generating a nonuniform discharge which carries the excitation out of the path of the gain probe beam. Taking the sound speed in the tube as 1000 $m\,s^{-1}$ we find a full wave period in the 2 cm tube of 20 μs, which is close to the observed period. The ratio, $JxB/p \cong 0.3\ m^{-1}$.

It is concluded that the peak values from traces such as these on Fig. 3.5 are the gains which would be realizable in a flow system. A series of such peak values are tabulated in Table 4 along with other parameters of the plasma. The peak gain values are plotted in Fig. 3.6.

It will be seen from Fig. 3.6 that the gain peaks with increasing magnetic field for fixed current density, CO_2 fraction and pressure. This is probably due to the pressure wave phenomenon discussed above. Since for fixed current the dissipation and hence the electron temperature increase with

increasing magnetic field, we would expect the gain also to increase, and gradually saturate.

The measured gains are quite large (by MHD laser standards) and in fact larger than the small signal gains cited in Section II. Reference to Table 4 shows that other plasma parameters are as expected for an MHD laser plasma. The apparent Hall parameter $\beta_{app} \simeq 0.5$ and decreases slightly with increasing magnetic field as expected for an eletrothermally unstable plasma . The conductivities and electron densities are in the expected range, much larger than for usual gas discharge laser plasmas.

A critical question is whether the electric field is in the range accessible by UxB action. For the magnetic field used in these experiments, and and a flow velocity of 3000 ms^{-1} (Mach number of 3) we estimate

$$UxB \simeq 1500 \text{ volt } m^{-1} = 15 \text{ volt } cm^{-1}$$

which is slightly below the measured values. Thus the magnetic field in an MHD laser using the experimental plasma conditions would have to be at least 1 tesla. At state of the art fields of 4 to 5 tesla the UxB field would be several times that required.

V. SUMMARY AND CONCLUSIONS

The fundamental mechanisms of lasing phenomena in MHD lasers are being studied by a combination of numerical modeling and a pulsed experimental simulation of the MHD flow laser. In the kinetic representation of the CO_2 a three level model is used which accounts for a finite coupling between the symmetric stretch and bending modes. The calculations using published coupling rates between these (100 → 020,010) levels indicate that the coupling may limit MHD laser output at 10.6 μ. It is conjectured that this limit can be avoided by oscillation at 9.6 μ. The pulsed experiment has demonstrated gain as high as 0.3 percent per cm at MHD laser conditions, with gas composition He + 0.0074 CO_2 + 10^{-5} Cs and total pressure 50 mm Hg. The current density was approximately 0.5 amp cm^{-2}, the electric field 20 volts cm^{-1} and the magnetic field 0.5 tesla. It is concluded that plasma conditions suitable for MHD laser operation have been achieved in the pulsed simulation. The numerical modeling indicates that these conditions can be reached in an MHD flow laser.

TABLE 1

SUMMARY OF REPORTED VALUES OF
$CO_2(10°0)$-$CO_2(01'0)$ RELAXATION RATE

Investigators	Rate ($atm^{-1}sec^{-1}$)
Rhodes, Kelly and Javan[14]	3.0×10^8
Carbone and Witteman[15]	6.8×10^6
Seeber[8]	3.4×10^7
Bulthuis and Ponsen[17]	9.9×10^6
Rosser, Hoag and Gerry[18]	7.6×10^5
Bulthuis[19]	7.7×10^6
Stark[20]	1.1×10^8
Jacobs, Pettipiece and Thomas[21]	$\simeq 10^7$
Murray, Mitchner and Kruger[22]	$0.9 - 1.5 \times 10^6$
This work (Section 4.1)	4.0×10^7

TABLE 2

COMPUTATIONAL RESULTS FROM TWO-TEMPERATURE MODEL

x (m)	Small Signal Gain (%/cm)	T_e	n_e (m^{-3})	T_{100}	T_{010}	T_{001}	T	U (m/sec)	I (kW/cm^2)	gI_3 (W/m^3)
0.000	-0.0087	-	-	1567.5	1567.5	1567.5	1567.5	2329.9	-	-
0.025	-0.0117	-	-	653.5	653.5	966.8	630.3	4190.5	-	-
0.050	0.0161	-	-	415.0	415.0	851.6	386.9	4486.1	-	-
0.075	0.0662	3240.8	8.88×10^{18}	507.9	507.9	1283.4	386.7	4484.7	25.3	1.67×10^{7}
0.100	0.0663	3493.1	1.14×10^{19}	564.6	564.6	1384.9	388.2	4482.1	34.0	2.20×10^{7}
0.150	0.0683	3433.1	3.51×10^{19}	802.5	802.5	1983.8	400.2	4465.4	75.3	5.00×10^{7}
0.200	0.0726	3149.4	3.64×10^{19}	800.5	800.5	2061.6	422.3	4441.6	63.0	4.14×10^{7}
0.250	0.0697	3136.2	3.63×10^{19}	794.7	794.7	2050.6	444.8	4417.6	60.2	3.97×10^{7}
0.300	0.0670	3133.8	3.61×10^{19}	791.3	791.3	2044.4	465.7	4395.3	58.2	3.84×10^{7}
0.350	0.0713	3142.6	3.60×10^{19}	786.6	786.6	2117.4	483.7	4375.8	51.0	3.33×10^{7}
0.400	0.0679	3132.0	3.59×10^{19}	783.5	783.5	2111.8	509.9	4347.6	47.9	3.13×10^{7}
0.450	0.0703	3144.6	3.58×10^{19}	780.2	780.2	2179.3	532.1	4323.6	39.9	2.65×10^{7}
0.500	0.0672	3133.1	3.57×10^{19}	782.4	782.4	2184.4	553.8	4300.2	35.2	2.33×10^{7}

TABLE 3

COMPUTATIONAL RESULTS FROM THREE-TEMPERATURE MODEL
RELAXATION RATES FROM MURRAY, MITCHNER AND KRUGER

x (m)	Small Signal Gain (%/cm)	T_e	n_e (m^{-3})	T_{100}	T_{010}	T_{001}	T	U (m/sec)	I (kW/cm^2)	gI_3 (W/m^3)
0.000	-0.0087	-	-	1567.5	1567.5	1567.5	1567.5	2329.9	-	-
0.025	-0.148	-	-	1466.7	516.2	1250.9	488.1	3867.8	-	-
0.050	-0.276	-	-	1359.5	328.2	1151.6	300.9	4111.9	-	-
0.075	-0.159	2911.8	8.60×10^{18}	1315.1	424.7	1486.9	300.5	4108.6	-	-
0.100	-0.036	3440.2	1.03×10^{19}	1273.7	452.5	1979.5	300.8	4100.7	-	-
0.150	0.0668	3288.5	4.07×10^{19}	1353.6	732.5	3089.1	311.1	4052.2	5.0	3.32×10^{6}
0.200	0.0664	3176.9	4.14×10^{19}	1329.6	736.0	3060.2	327.6	3980.4	2.5	1.65×10^{6}
0.250	0.0660	3161.5	4.16×10^{19}	1304.4	740.7	3027.1	343.3	3909.2	2.7	1.79×10^{6}
0.300	0.0666	3148.5	4.18×10^{19}	1278.4	744.0	3003.9	357.7	3840.2	2.7	1.75×10^{6}
0.350	0.0667	3128.4	4.20×10^{19}	1255.0	740.3	2971.4	372.3	3766.8	2.7	1.77×10^{6}
0.400	0.0667	3100.9	4.21×10^{19}	1233.1	730.3	2930.4	386.8	3688.4	2.7	1.79×10^{6}
0.450	0.0667	3067.1	4.20×10^{19}	1211.0	719.6	2884.4	399.7	3613.2	2.7	1.78×10^{6}
0.500	0.0660	3009.7	4.14×10^{19}	1184.2	707.5	2814.1	413.6	3523.8	2.6	1.71×10^{6}

TABLE 4

Exp. No.	Peak Gain α % cm^{-1}	Axial Field Volts/cm	Axial Current Amp/cm^2	Axial Cond. mho/m	β_{app}	B Field Tesla	n_e m^{-3}
3048	0.136	19.6	0.68	3.45	0.0	0.0	4.6×10^{18}
3049	0.166	16.8	0.62	3.69	0.54	0.28	4.6×10^{18}
3050	0.32 ±0.04	18.2	0.62	3.41	0.50	0.42	4.1×10^{18}
3051	0.10 ±0.03	21.7	0.62	2.86	0.41	0.56	3.63×10^{18}

$n_{He} = 1.5 \times 10^{24} m^{-3}$; $f_{CO_2} = 0.8\%$; $f_{Cs} = (4.0 \pm 1.5) \times 10^{-6}$

FIGURE 2.1 - TEMPERATURE RESPONSE PROFILES FOR TWO-TEMPERATURE CO_2 MODEL

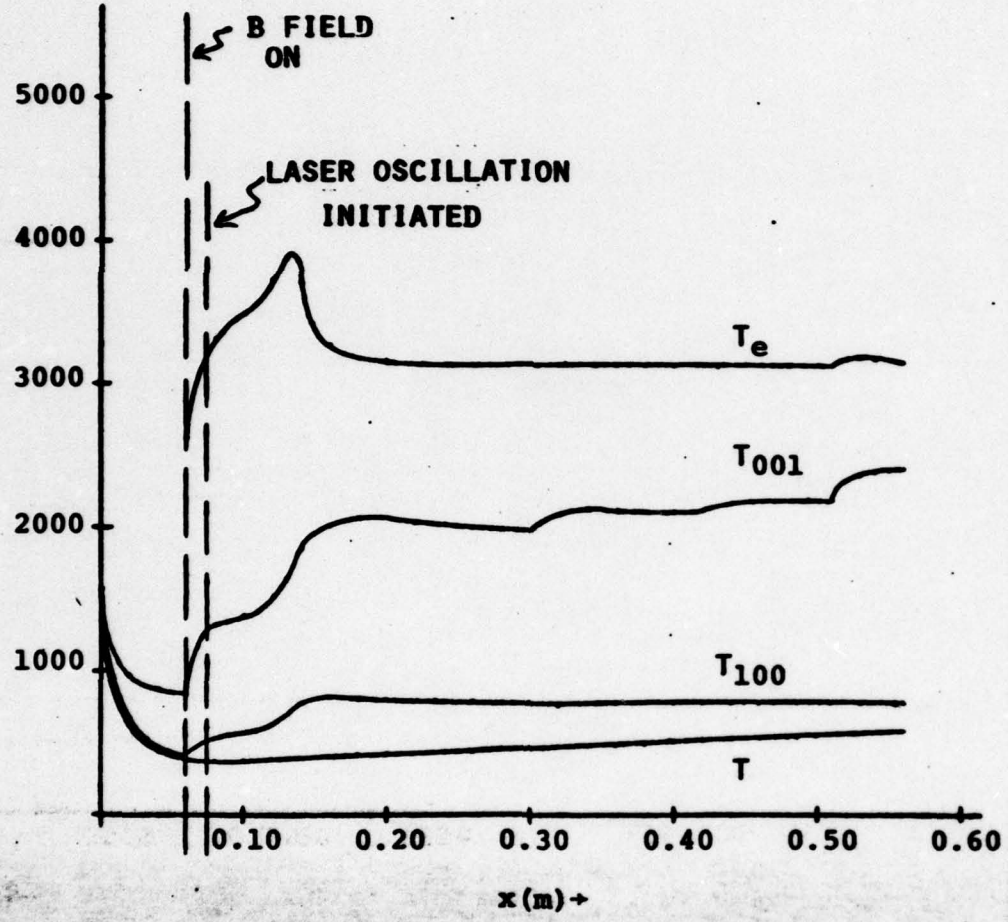

FIGURE 2.2 - TEMPERATURE RESPONSE PROFILES FOR THREE-TEMPERATURE CO_2 MODEL

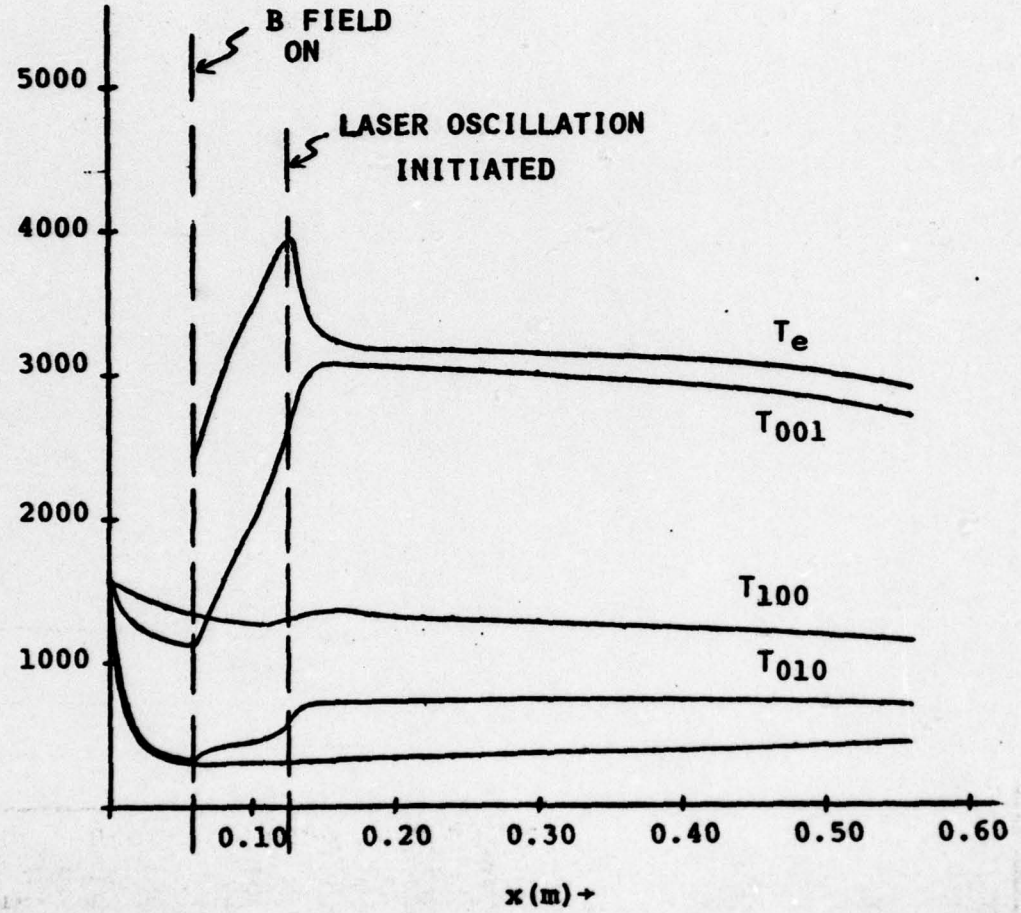

FIGURE 2.3 - COMPARISON OF OPTICAL POWER DENSITY IN TWO- AND THREE-TEMPERATURE MODELS

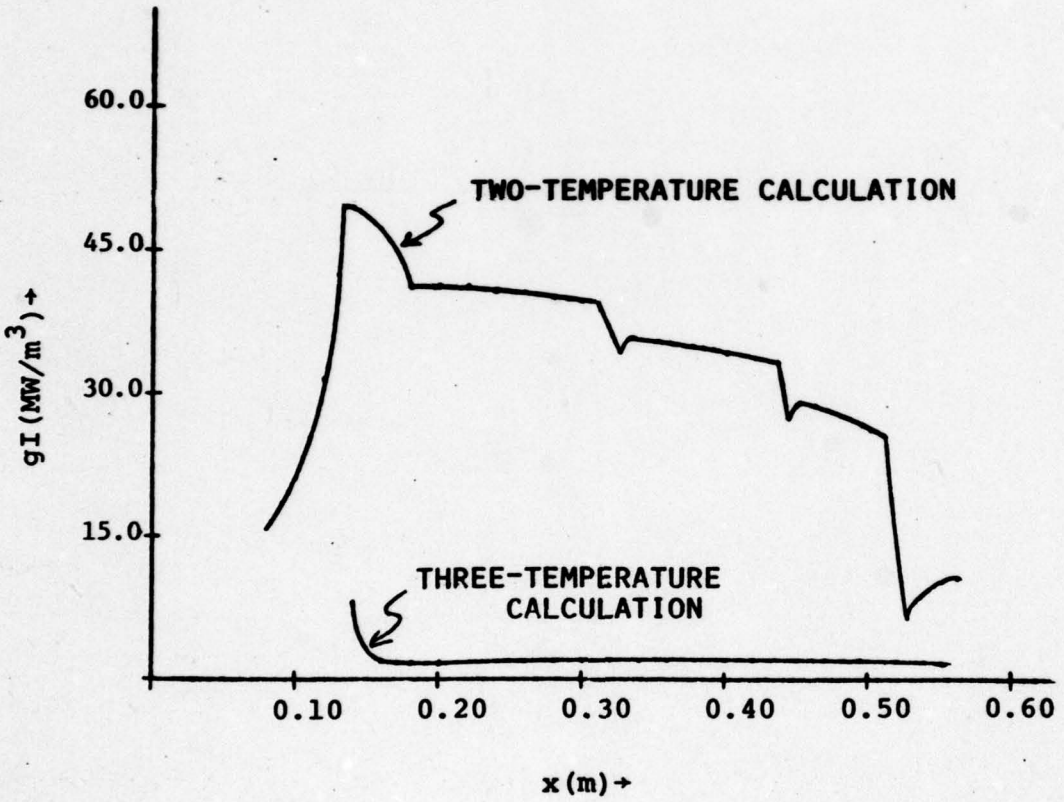

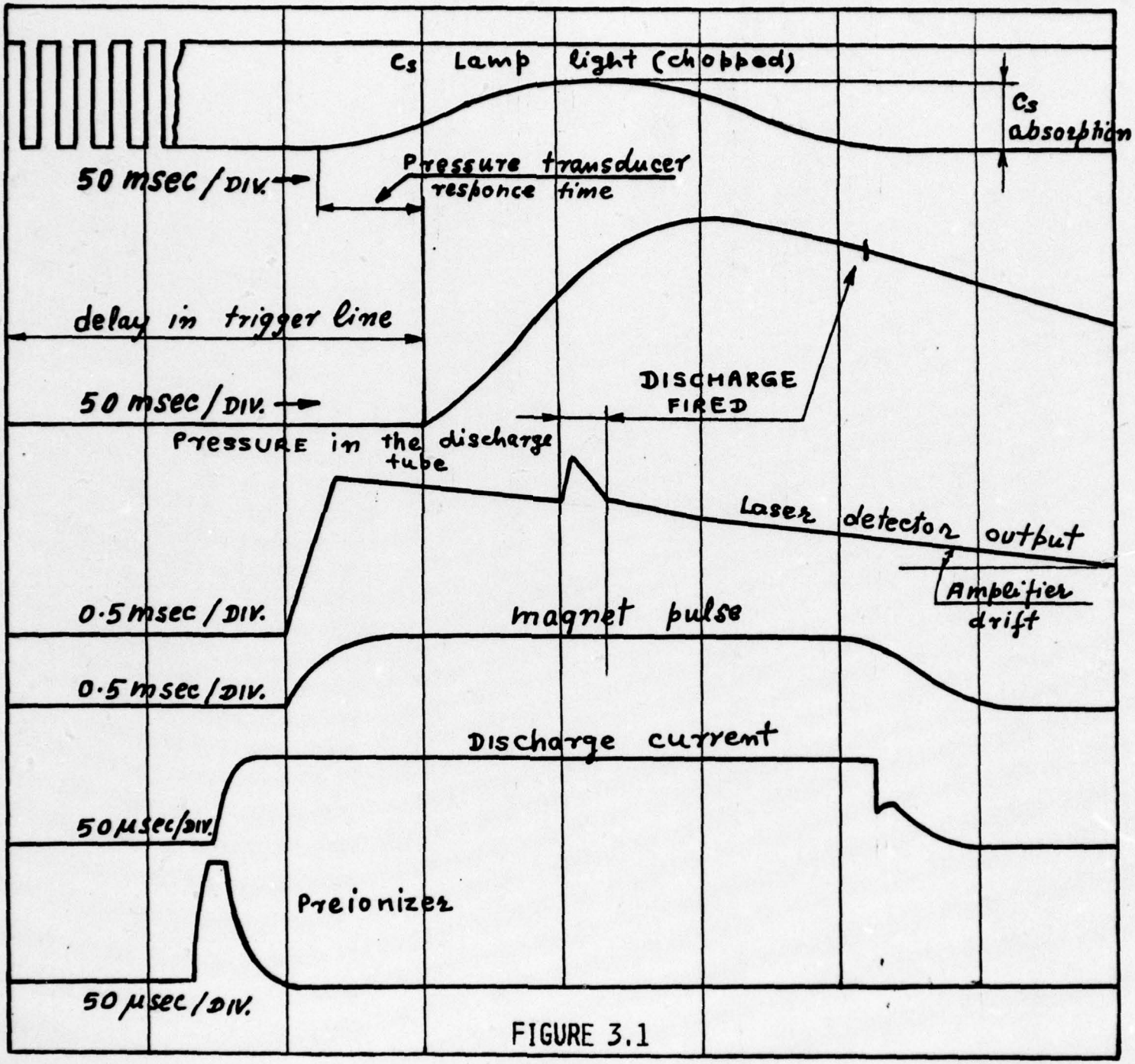
Cs Lamp light (chopped)
Cs absorption
50 msec / DIV.
Pressure transducer responce time
delay in trigger line
50 msec / DIV.
DISCHARGE FIRED
PRESSURE in the discharge tube
Laser detector output
Amplifier drift
0.5 msec / DIV.
magnet pulse
0.5 msec / DIV.
Discharge current
50 μsec/DIV.
Preionizer
50 μsec / DIV.

FIGURE 3.1

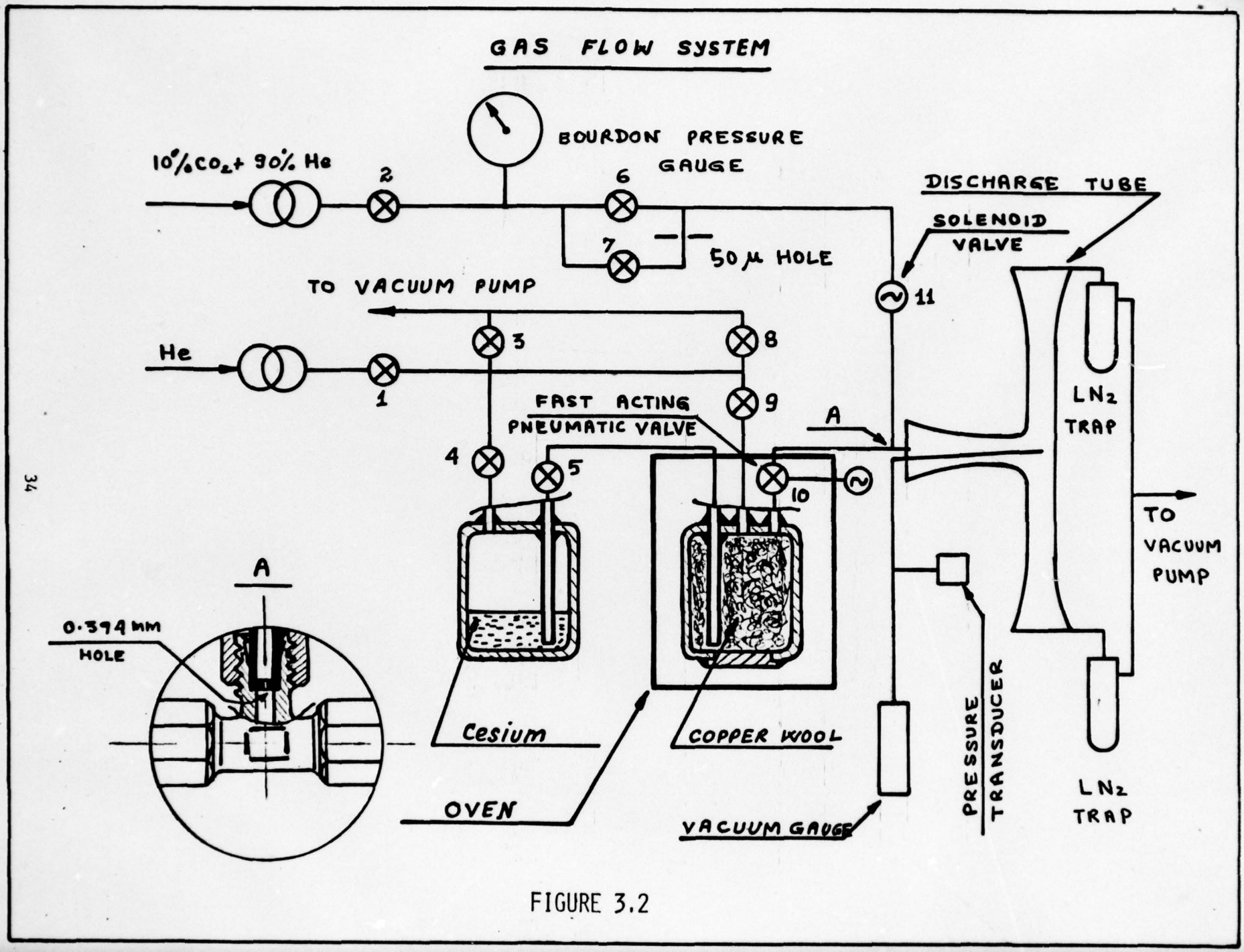
GAS FLOW SYSTEM
BOURDON PRESSURE GAUGE
10% CO_2 + 90% He
2
6
DISCHARGE TUBE
SOLENOID VALVE
7
50 μ HOLE
TO VACUUM PUMP
11
He
3
8
1
9
FAST ACTING PNEUMATIC VALVE
A
LN_2 TRAP
4
5
10
TO VACUUM PUMP
A
0.394 mm HOLE
Cesium
COPPER WOOL
OVEN
VACUUM GAUGE
PRESSURE TRANSDUCER
LN_2 TRAP

FIGURE 3.2

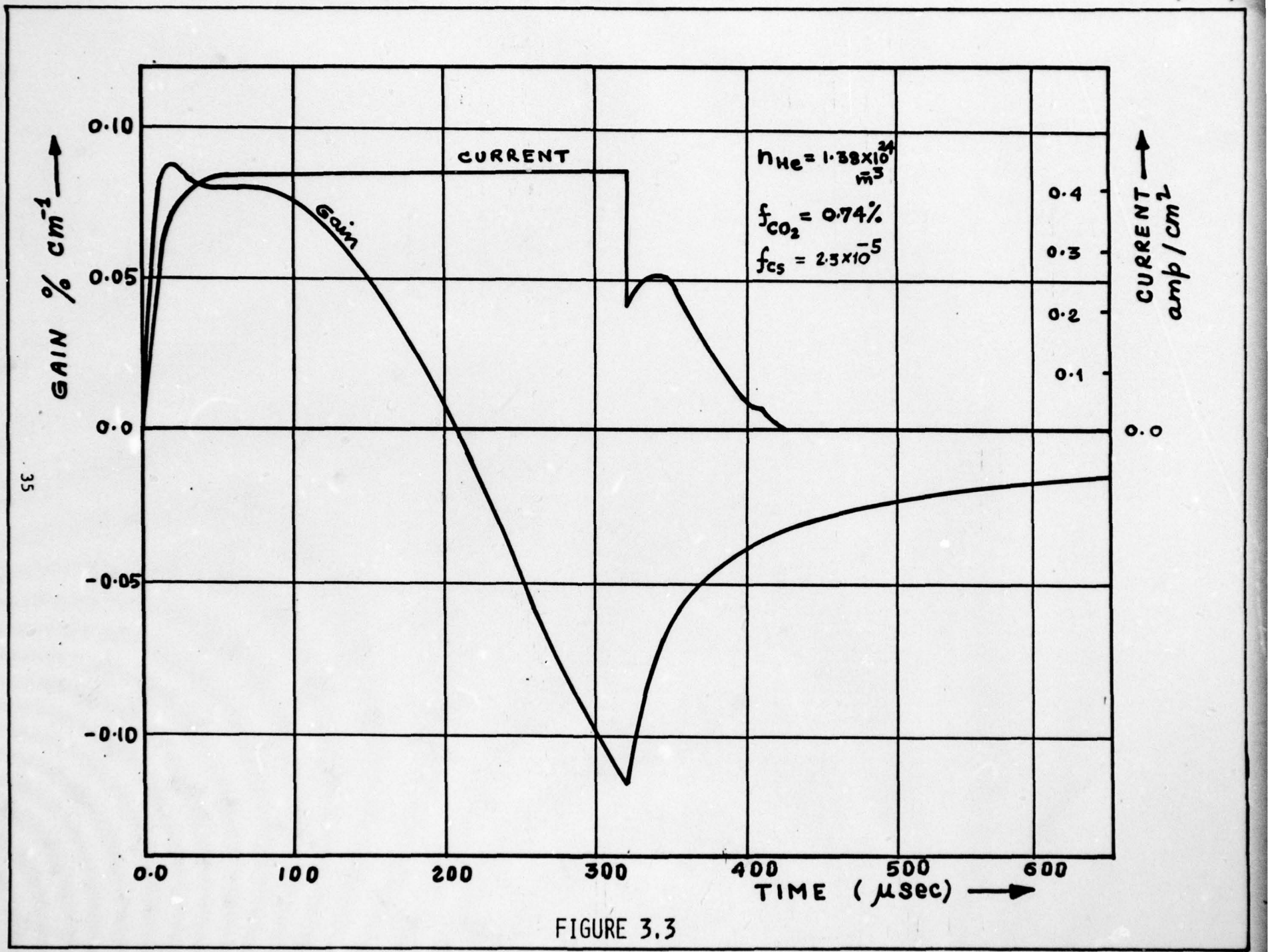
GAIN % cm⁻¹
0.10
0.05
0.0
-0.05
-0.10
CURRENT
Gain
$n_{He} = 1.38 \times 10^{24}$ m⁻³
$f_{CO_2} = 0.74\%$
$f_{CS} = 2.5 \times 10^{-5}$
0.4
0.3
0.2
0.1
0.0
CURRENT → amp/cm²
0.0
100
200
300
400
500
600
TIME (μsec) →

FIGURE 3.3

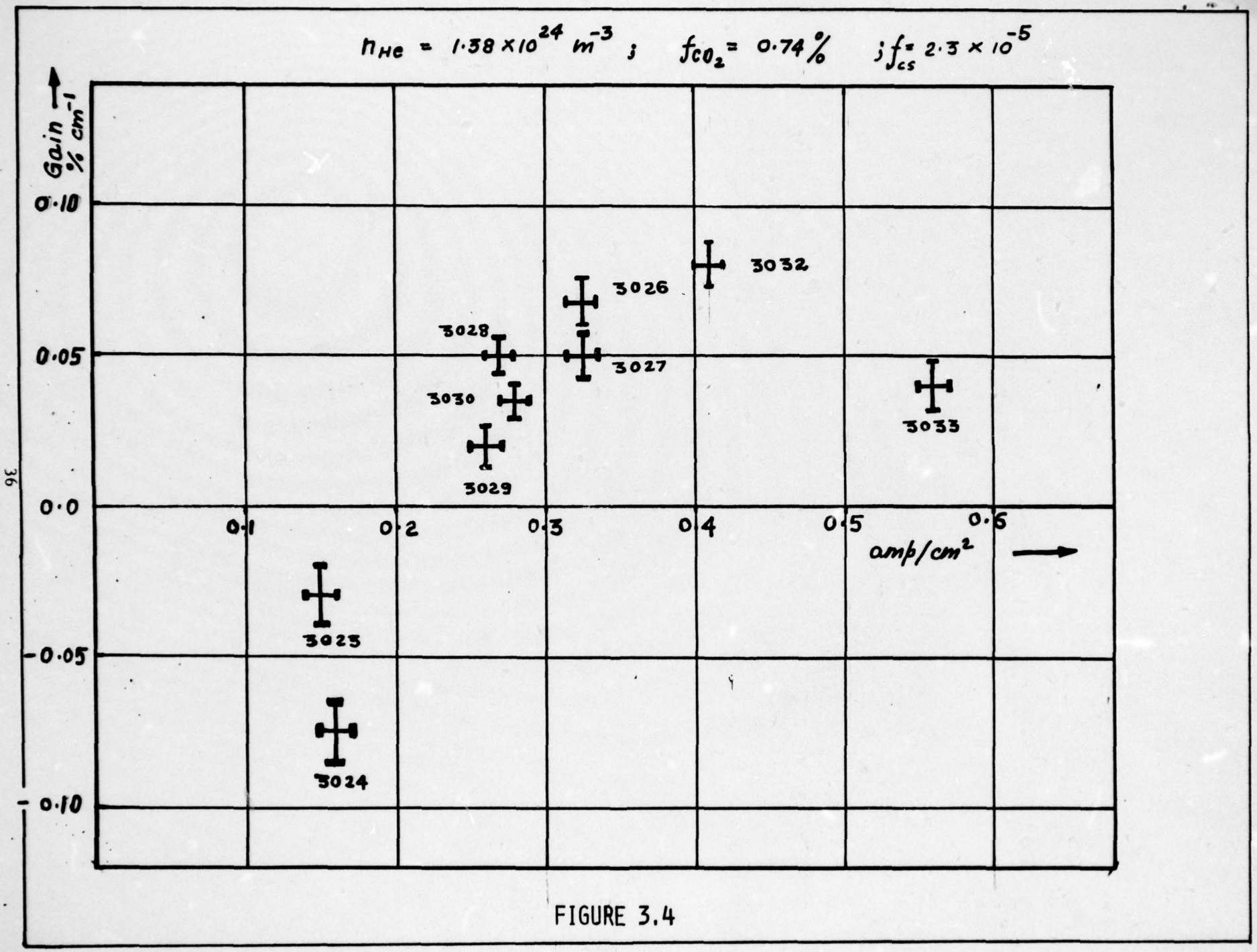
$n_{He} = 1.38 \times 10^{24}\ m^{-3}$; $f_{CO_2} = 0.74\%$; $f_{cs} = 2.3 \times 10^{-5}$
Gain — % cm⁻¹
0·10
0·05
0·0
-0·05
-0·10
0·1
0·2
0·3
0·4
0·5
0·6
amp/cm²
3024
3025
3026
3027
3028
3029
3030
3032
3033

FIGURE 3.4

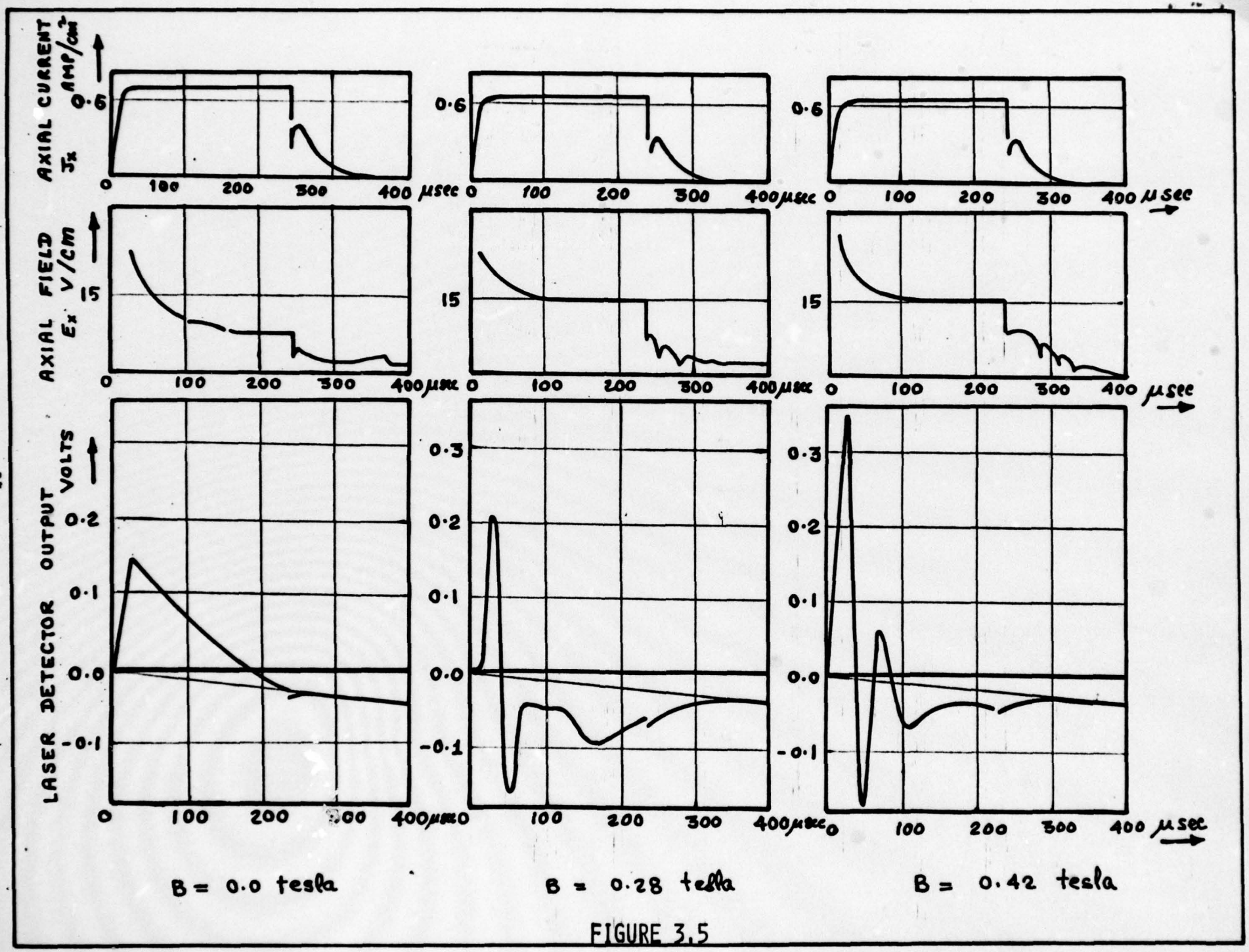
AXIAL CURRENT Jx AMP/cm²
0.6
0 100 200 300 400 μsec
AXIAL FIELD Ex V/cm
15
0 100 200 300 400 μsec
LASER DETECTOR OUTPUT VOLTS
0.3
0.2
0.1
0.0
-0.1
0 100 200 300 400 μsec
B = 0.0 tesla
B = 0.28 tesla
B = 0.42 tesla

FIGURE 3.5

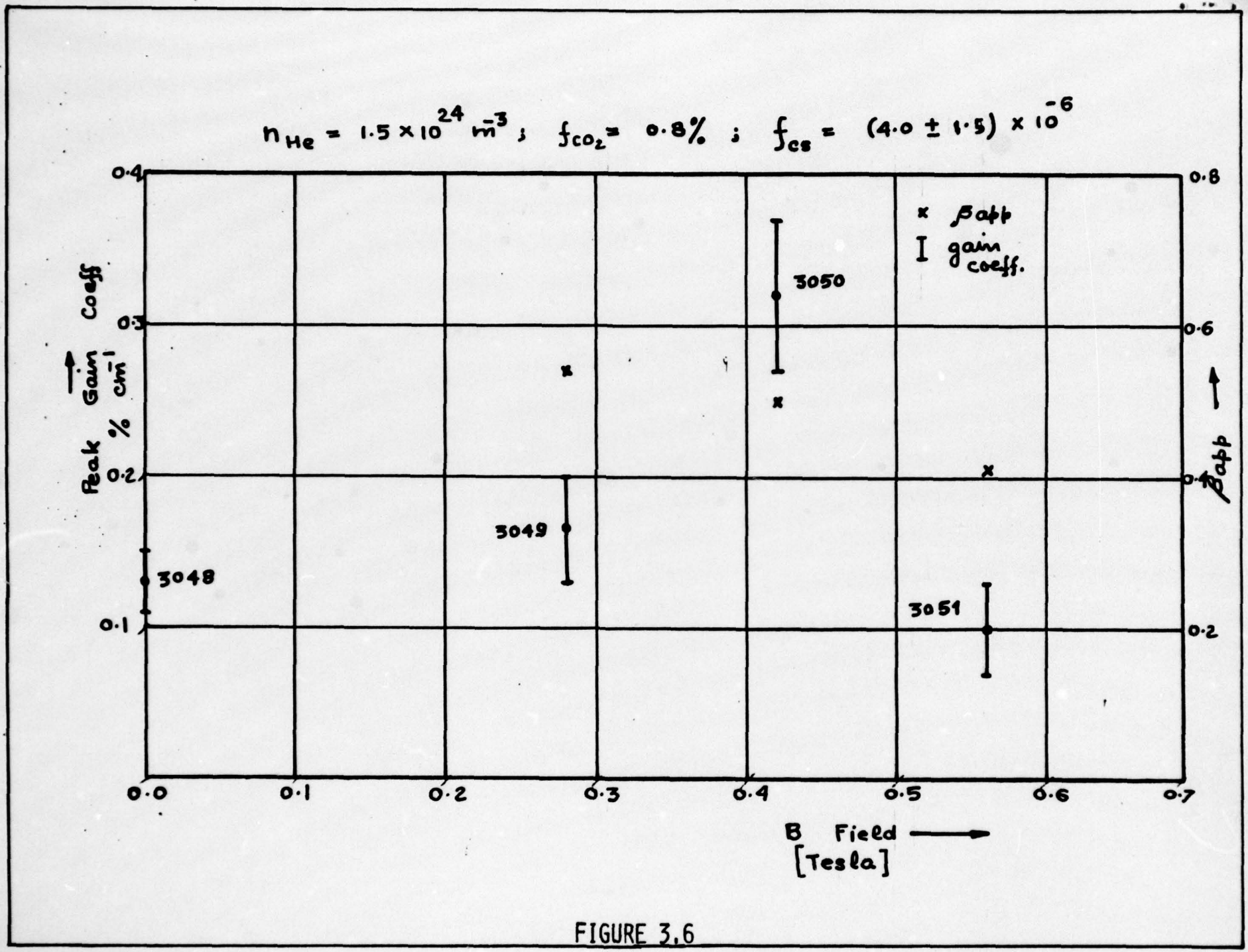
$n_{He} = 1.5 \times 10^{24}\ m^{-3}$; $f_{CO_2} = 0.8\%$; $f_{Cs} = (4.0 \pm 1.5) \times 10^{-6}$
Peak Gain Coeff % cm⁻¹
βapp
x βapp
I gain coeff.
3048
3049
3050
3051
0.4
0.3
0.2
0.1
0.8
0.6
0.4
0.2
0.0
0.1
0.2
0.3
0.4
0.5
0.6
0.7
B Field [Tesla]

FIGURE 3.6

References

1. Kerrebrock, J.L., "Fundamental Mechanisms of Nonequilibrium MHD Lasing Phenomena," Final Scientific Report AFOSR-74-2680, Oct. 1976 M.I.T. Gas Turbine & Plasma Dynamics Lab.

2. Hsu, M.S.S., "Experimental Investigation of a Nonequilibrium Magnetohydrodynamic Generator with Slanted Electrode Walls," Ph.D. Thesis, M.I.T., June (1971).

3. Draper, J.S., and Kerrebrock, J.L., "Molecular Behavior in Nonequilibrium MHD Generators," 5th Int. Conf. on MHD Elec. Power Gen., Munich (1971).

4. Brown, R.T., Hall, R.J., and Nighan, W.L., "Laser Excitation Using a Nonequilibrium MHD Generator," United Aircraft Research Lab. Report, East Hartford, CT (1969).

5. Kerrebrock, J.L., and Dethlefsen, R., "Experimental Investigation of Fluctuations in a Nonequilibrium Plasma," J. AIAA, 6, 11, 2115, Nov. (1968).

6. Solbes, A., "Quasi-Linear Plane Wave Study of Electrothermal Instabilities," SM-107/26, 4th Int. Conf. on MHD Elec. Power Gen., Warsaw (1968).

7. Louis, J.F., "Studies of a Disk Hall Generator Driven in a Shock Tunnel," 8th Symp. on Eng. Aspects of MHD, Stanford (1967).

8. Oliver, D.A., Solbes, A., Kerrebrock, J.L., et al., "Ionization Instabilities and Discharge Characteristics of an MHD Laser," 12th Symp. on Eng. Aspects of MHD, Argonne, Illinois, March (1972).

9. Lowenstein, A., "Physical Processes in a Magnetohydrodynamic Laser," Ph.D. Thesis, M.I.T., Feb. (1974).

10. Biberman, L.M., Vorobjev, V.S., Ivanov, R.S., et al., "Some Results of MHD-Laser Investigation," Proc. 16th Symp. on Eng. Aspects of MHD, Pittsburgh, PA (1977).

11. Nighan, W.L., and Brown, R.T., "Laser Excitation Using a Nonequilibrium MHD Generator," AIAA Paper 71-67 (1971).

12. Bullis, R.H., Churchill,T.L., Nigham, W.L., et al., Investigation of the Feasibility of a Magnetohydrodynamic Laser," Report #N921308-4, United Aircraft Research Lab., East Hartford, CT, May (1974).

13. Anderson, Jr, John D., Introduction to Gasdynamic Lasers, Academic Press, NY, NY (1976).

14. Rhodes, C.K., Kelly, M.J., and Javan, A., "Collisional Relaxation of the 100 State in Pure CO_2," J. Chem. Phys., 48, 5730 (1968).

15. Carbone, R.J., and Wittenman, W.J., "Vibrational Energy Transfer in CO_2 Under Laser Conditions With and Without Water Vapor," IEEE J. Q. Elec.,QE-5, 422 (1969).

16. Seeber, K.N., "Radiative and Collisional Transitions Between Coupled Vibrational Modes of CO_2," J. Chem. Phys., 55, 10, 5077 (1971).

17. Bulthuis, K., and Ponsen, G.J., "On the Relaxation of the Lower Laser Level of CO_2," Chem. Phys. Let., 14, 5, 613 (1972).

18. Rosser, Jr., W.A., Wood, R.E., and Gerry, E.T., "Relaxation of Excess Populations in the Lower Laser Level CO_2 (100)," J. Chem Phys. 57, 10, 4153 (1972).

19. Bulthuis, K., "Laser Power and Vibrational Energy Transfer in CO_2 Lasers," J. Chem. Phys., 58, 12, 5786 (1973).

20. Stark, E.E., "Measurement of the 100-020 Relaxation Rate in CO_2," Appl. Phys. Let., 23, 6 335 (1973).

21. Jacobs, Ralph R., Pettipiece, Kenneth, J., and Thomas, Scott J., "Rate Constants For the CO_2 02°0-10°0 Relaxation," Phys. Rev. A, 11, 1, 54 (1975).

22. Murray, Edward R., Kruger, Charles H., and Mitchner, Morton, "Vibrational Nonequilibrium in Carbon Dioxide Electric Discharge Lasers," J. Chem. Phys., 62, 2, 388 (1975).

23. Parma, Cesare, "Study of the M.I.T. Non-Equilibrium MHD Generator Experiments," S.M. Thesis, M.I.T. Dept. of Aero. & Astro., May (1974).

24. Cole, James A., "A Numerical Study of Non-Equilibirum MHD Generators," S.M. Thesis, M.I.T. Dept. of Aero. & Astro., May (1976).

25. Kerrebrock, Jack L., "Nonequilibrium Ionization Due to Electron Heating: I. Theory," AIAA J., 2, 6, 1072, June (1964).

26. Solbes, A., "Instabilities in Non-Equilibrium MHD Plasmas, A Review," AIAA Paper 70-40 (1970).

27. Solbes, A., "Study of Non-Equilibrium MHD Generator Flows with Strong Interaction," Final Report for NSF P3K0488-00, June (1974).

28. Christiansen, Walter H., and Tsongas, George A., "Gain Kinetics of CO_2 Gasdynamic Laser Mixtures at High Pressure," Phys. Fluids 14, 12 December (1971).